

p53-Regulated Increase in Oxidative-Stress–Induced Apoptosis in Fuchs Endothelial Corneal Dystrophy: A Native Tissue Model

Bebrooz Azizi, Alireza Ziaei, Thomas Fuchsluger, Thore Schmedt, Yuming Chen, and Ula V. Jurkunas

PURPOSE. This study compared susceptibility of Fuchs endothelial corneal dystrophy (FECD) and normal corneal endothelial cells (CECs) to oxidative stress, and studied the mechanism of oxidative-stress–induced apoptosis in FECD-affected endothelium.

METHODS. For in vitro studies, immortalized normal and FECD human corneal endothelial cell lines (HCECi and FECDi, respectively) were exposed to *tert*-butyl hydroperoxide (tBHP). Apoptotic cell populations were distinguished using flow cytometry. Reactive oxygen species production was measured by a horseradish peroxidase assay. For ex vivo studies, CECs were exposed to tBHP. Oxidative DNA damage and apoptosis were assessed by anti-8-hydroxydeoxyguanosine antibody and TUNEL assay, respectively. p53 and phospho-p53 levels were assessed by Western blot and immunohistochemistry.

RESULTS. Flow cytometry revealed a higher rate of apoptosis in FECDi than that in HCECi after exposure to 0.5 mM ($P = 0.010$) and 1.0 mM tBHP ($P = 0.041$). Further analysis showed increased production of H_2O_2 by FECDi than that by HCECi. Oxidative DNA damage increased in both normal and FECD CECs after exposure to 0.5 mM tBHP ($P = 0.031$ and 0.022 , respectively), leading to a 21% increase in TUNEL-positive CECs in FECD ($P = 0.015$) but no change in normal. Baseline p53 expression was twofold higher in FECD than that in normal endothelium ($P = 0.002$). Immunofluorescence revealed an increase in p53 and phospho-p53 levels in FECD compared with that in normal endothelium.

CONCLUSIONS. FECD CECs are more susceptible to oxidative DNA damage and oxidative-stress–induced apoptosis than normal. Increased activation of p53 in FECD suggests that it mediates cell death in susceptible CECs. The authors conclude that p53 plays a critical role in complex mechanisms regulating oxidative-stress–induced apoptosis in FECD. (*Invest Ophthalmol Vis Sci.* 2011;52:9291–9297) DOI:10.1167/iovs.11-8312

From the Schepens Eye Research Institute, Massachusetts Eye and Ear Infirmary, Department of Ophthalmology, Harvard Medical School, Boston, Massachusetts.

Supported in part by an award from the Eye Bank Association (BA and TS); National Eye Institute/National Institutes of Health Grant R01 EY20581; and a Research to Prevent Blindness Award (UVJ).

Submitted for publication July 28, 2011; revised October 19, 2011; accepted November 1, 2011.

Disclosure: **B. Azizi**, None; **A. Ziaei**, None; **T. Fuchsluger**, None; **T. Schmedt**, None; **Y. Chen**, None; **U.V. Jurkunas**, None

Corresponding author: Ula V. Jurkunas, Schepens Eye Research Institute, 20 Staniford Street, Boston, MA 02114; ula_jurkunas@meei.harvard.edu.

Fuchs endothelial corneal dystrophy (FECD) is characterized by progressive loss of corneal endothelial cells (CECs) and concomitant accumulation of extracellular matrix deposits in the form of guttae. As the disease progresses, the endothelial cell number becomes critically low and, by virtue of decreased endothelial pump and/or barrier functions, the cornea is no longer able to maintain its state of relative deturgescence, and corneal edema ensues. In the past decade, apoptotic cell death has been demonstrated in FECD endothelium, as seen by terminal deoxynucleotide transferase dUTP nick end labeling (TUNEL) and DNA fragmentation assays.^{1,2}

One of the major inducers of cellular apoptosis is macromolecular damage (including DNA) due to oxidative stress. Several well-described disease processes have been associated with apoptosis involving oxidative stress: amyotrophic lateral sclerosis, Alzheimer's disease, Parkinson's disease, Huntington's disease, age-related macular degeneration, and aging. We recently reported findings that place FECD in the category of oxidative-stress–related disorders as well.^{3,4} These studies demonstrated an oxidant–antioxidant imbalance and accumulation of oxidized DNA lesions in FECD endothelium compared with normal corneal endothelium.^{3,4} Specifically, PCR array detected transcriptional downregulation of peroxiredoxins, thioredoxin reductase, superoxide dismutase isoforms, and metallothionein without compensatory upregulation of catalase and glutathione-dependent antioxidants. Immunocytochemical studies showed colocalization of apoptotic cell death and oxidative DNA damage in FECD CECs.

Despite these findings, it is unclear whether oxidative stress is a cause of apoptosis in FECD CECs. In this study, we hypothesized that oxidant–antioxidant imbalance renders FECD corneal endothelium more susceptible to oxidative-stress–induced apoptotic cell death. To investigate this hypothesis, we used two model systems: (1) immortalized normal and FECD corneal endothelial cell lines and (2) native samples from FECD patients and normal cadavers. The latter system enabled us to study tissues under conditions simulating an in vivo environment, in that cellular response to pro-oxidant treatments was investigated in native human endothelium attached to Descemet's membrane (DM) for both FECD and normal controls. In addition, we used E6/E7-transformed, immortalized normal and FECD corneal endothelial cell lines, designated HCECi and FECDi, respectively. After pro-oxidant treatments, we compared cellular responses in normal and diseased CECs, and we related the native sample data to the cell line data. We detected altered resistance of FECD endothelium to oxidative stress and a higher rate of apoptosis than that in normal endothelium. Moreover, p53 and phosphorylated (activated) p53 (phospho-p53), a transcription factor involved in oxida-

tive-stress-induced apoptosis, was shown to play an important role in cell death seen in FECD.

MATERIALS AND METHODS

Human Tissue

This study adhered to the tenets of the Declaration of Helsinki and was approved by the institutional review boards of both the Massachusetts Eye and Ear Infirmary and Schepens Eye Research Institute. Written, informed consent was obtained from patients undergoing surgical treatment for FECD. After surgical removal, the tissue was immediately placed in storage medium (Optisol-GS; Bausch & Lomb, Rochester, NY) at 4°C. Normal human corneal buttons obtained from Tissue Banks International (Baltimore, MD) and National Disease Research Interchange (Philadelphia, PA) were used as controls. We used previously published criteria to determine donor tissue suitability.⁵ The corneal endothelial cell layer, along with DM, were dissected from the stroma of the corneal buttons under a dissecting microscope. Table 1 presents information regarding the tissue samples used. Normal donors were sex- and decade-matched with FECD donors.

Induction of Oxidative Stress

Oxidative stress was induced by *tert*-butyl hydroperoxide (tBHP; Sigma-Aldrich, St. Louis, MO), diluted in serum-free low-glucose Dulbecco's modified Eagle's medium (DMEM; Invitrogen, Carlsbad, CA) to final concentrations of 0 to 1 mM.

Immunocytochemistry

Human tissue samples were placed in 0 to 1 mM tBHP diluted in DMEM at room temperature. After 4 hours of exposure to oxidative stress, immunocytochemistry was performed on the samples as previously described.⁵ Briefly, after fixation, tissues were permeabilized and blocked in 5% donkey serum. Tissues were then stained with anti-8-hydroxydeoxyguanosine (8-OHdG; Millipore, Billerica, MA), anti-p53 (Santa Cruz Biotechnology, Santa Cruz, CA), anti-phospho-p53 (Ser15) (Cell Signaling Technology, Danvers, MA), followed by incubation with appropriate secondary antibody and TO-PRO-3 iodide (Molecular Probes, Eugene, OR). Apoptosis was detected by TUNEL assay (In Situ Cell Death Detection Kit; Roche Diagnostics, San Francisco, CA) according to the manufacturer's instructions. Digital images were obtained using a spectral photometric confocal microscope (Leica DM6000S with LCS 1.3.1 software; Leica Camera AG, Solms, Germany). Total and p53 or TUNEL-positive CECs were counted using particle analysis and cell counter plug-ins with ImageJ software (developed by Wayne Rasband, National Institutes of Health, Bethesda, MD; available at <http://rsb.info.nih.gov/ij/index/html>), respectively. Fluorescently labeled 8-OHdG was quantified by dividing integrated fluorescence intensity (obtained by ImageJ, NIH) by the total number of cells.

Western Blot Analysis

Normal and FECD specimens were placed in radioimmunoprecipitation assay buffer (Cell Signaling Technology) supplemented with 50 mM sodium fluoride (New England BioLabs, Ipswich, MA), 1 mM sodium orthovanadate (New England BioLabs), and protease inhibitor cocktail tablet (Roche Diagnostics). Western blot was per-

formed using a previously described method.³ Briefly, proteins were separated by gel electrophoresis using 10% Bis-Tris gel (NuPAGE; Invitrogen), and transferred to polyvinylidene difluoride membrane. Blots were blocked with 5% nonfat milk and 2.5% bovine serum albumin in TTBS (50 mM Tris, pH 7.5, 0.9% NaCl₂, and 0.1% Tween-20) for 1 hour at room temperature and then incubated overnight with a primary antibody against p53 (1:200; Santa Cruz Biotechnology). The membranes were washed with TTBS and then incubated for 1 hour with horseradish peroxidase-conjugated anti-goat antibody (1:2000; Santa Cruz Biotechnology). Mouse anti-β-actin (1:4000; Sigma-Aldrich) was used to normalize protein loading. Proteins were detected with an enhanced chemiluminescence detection kit (Thermo Scientific, Pittsburgh, PA). Densitometry was performed with ImageJ software (NIH).

Human Corneal Endothelial Cell Culture

Normal⁶ and FECD⁷ human corneal endothelial cell lines (HCEC1 and FECD1, respectively), immortalized by infection with an amphotropic recombinant retrovirus containing human papilloma virus type 16 genes E6 and E7, were generous gifts of Dr. May Griffith (Ottawa Hospital Research Institute, Ottawa, Ontario, Canada) and Dr. Rajiv Mohan (University of Missouri Health System, School of Medicine, Columbia, MO). Cells were grown in T75 culture flasks in Chen's medium⁸ before use for flow cytometric studies.

Flow Cytometry

HCEC1 and FECD1 were harvested from T75 culture flasks and seeded in 12-well plates filled with Chen's medium. After cells became confluent, Chen's medium was replaced with 0 to 1 mM tBHP diluted in DMEM (Invitrogen) and incubated for 4 and 14 hours at 37°C in 5% CO₂. At the end of the treatment, cell culture media was removed and all wells were rinsed with PBS. Cells were then trypsinized and transferred to cell culture multflasks (Falcon tubes; BD Biosciences, San Jose, CA). After the cells were spun, the trypsin was discarded and the cells were washed with cold PBS. Cells in each tube were then resuspended in binding buffer and incubated with the plasma protein Annexin V (Ann) and propidium iodide (PI), in the dark, for 15 minutes, on ice (ApoptNexin FITC Apoptosis Detection Kit; Millipore). Ann is a member of the phosphatidyl-binding protein family, with strong affinity to phosphatidyl-serine. The counterstain PI was used to assay for cell membrane permeability (lysis). Cells in viable populations are in metabolically active stages of apoptosis and will stain for Ann but not PI, which is a DNA-binding dye. Late apoptotic populations are detected by binding both Ann and PI, whereas staining with PI alone indicates necrosis. Vital (Ann−/PI−), early apoptotic (Ann+/PI−), late apoptotic (Ann+/PI+), and necrotic (Ann−/PI+) cell populations were distinguished using a flow cytometer (BD LSR II cytometer; BD Biosciences).

Measurement of Reactive Oxygen Species Release

HCEC1 and FECD1 were seeded at a 150,000 cells per well density and grown for 20 hours in FNC (fibronectin type III repeat C of human tenascin-C)-coated (Athena Environmental Sciences, Inc., Baltimore, MD) 12-well plates to form a confluent monolayer. All subsequent steps were carried out in phenol red-free low-glucose DMEM (Invitrogen) medium, supplemented with 4 mM L-glutamine. Cells were washed and oxidative stress was induced by addition of 500 μM tBHP for 1 hour at 37°C. Control cells were kept in medium alone. Hydrogen peroxide released from normal and FECD corneal endothelial cells was detected using a horseradish peroxidase assay (Amplex Red; Invitrogen). After the treatment, the cells were washed once and further incubated at 37°C in medium containing 100 μM Amplex Red and 0.2 U/mL horseradish peroxidase. Oxidation of the Amplex Red by horseradish peroxidase in the presence of H₂O₂ yields highly fluorescent resorufin. Resorufin fluorescence in the cell supernatant was measured using a microplate reader (Synergy 2; BioTek, Winooski, VT) at excitation and emission wavelengths of 530 and 590 nm, respectively. To

TABLE 1. Donor Information

Factor	FECD	Normal
Average age, y*	70 ± 10	70 ± 10
Sex, female/male	8/3	13/9

* Average age with SD.

detect hydrogen peroxide release, resorufin fluorescence in the cell supernatant was read at the time points of 0, 20, 40, and 60 minutes, in a continuous fashion. Background fluorescence was corrected by subtracting the values derived from media alone. All measurements were done in triplicate.

Statistical Analysis

Statistical analyses were performed using commercial statistical analysis software (SPSS 16.0; SPSS, Inc., Chicago, IL). Paired Student's *t*-test was used to analyze corneas from the same donors and independent Student's *t*-test was used to compare normal and FECD specimens. Results are expressed as mean \pm SEM and considered significant if $P < 0.05$.

RESULTS

Increased Susceptibility of FECD CECs to Oxidative Stress In Vitro

To investigate the role of oxidative-stress-induced apoptosis, previously established normal⁶ and FECD⁷ corneal endothelial cell lines (HCECi and FECDi, respectively) were treated with increasing concentrations of tBHP (0–1 mM), and apoptotic cell populations were quantified using flow cytometry. After the 4-hour treatment with tBHP, the percentage of early apoptotic cells was similar in both HCECi and FECDi (Fig. 1A). However, after the 14-hour treatment with high concentrations of tBHP, a significantly higher rate of apoptosis was detected in

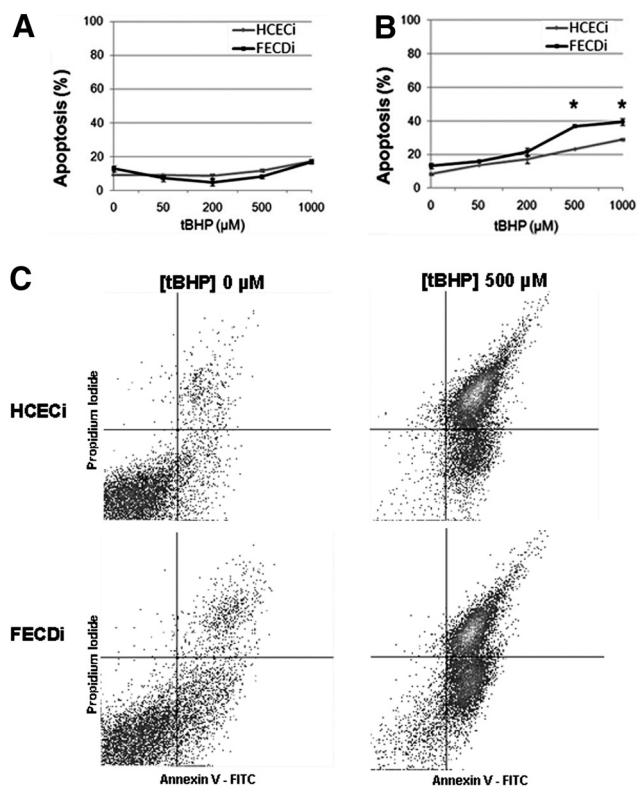


FIGURE 1. Normal and FECD immortalized cell lines (HCECi and FECDi, respectively) were treated with increasing concentrations of tBHP and stained with Annexin V (Ann) and PI. Early apoptosis (Ann+/PI-) was measured using quantitative flow cytometry. The 4-hour treatment (A) resulted in similar levels of apoptotic cells in both HCECi and FECDi. However, the 14-hour treatment (B) resulted in significantly higher apoptosis in FECDi ($*P < 0.05$). (C) A representative image of flow cytometric analysis of HCECi and FECDi treated with 500 μ M tBHP for 14 hours is illustrated.

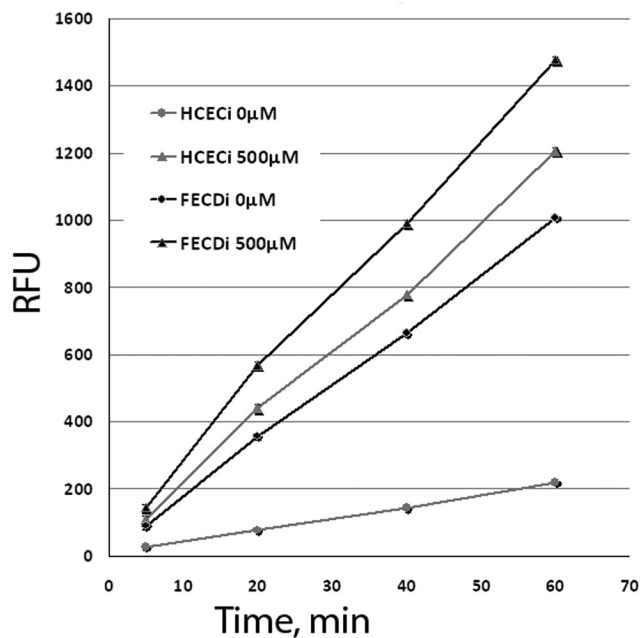


FIGURE 2. Hydrogen peroxide release from HCECi and FECDi measured using Amplex Red to detect resorufin fluorescence in the cell supernatants. The cells were treated with tBHP, and H_2O_2 release was detected at different time points as measured by relative fluorescence units (RFUs). All measurements were performed in triplicate. FECDi released a significantly higher level of H_2O_2 than did HCECi after 20, 40, and 60 minutes of incubation in both untreated (0 μ M) and treated (500 μ M) conditions. $*P < 0.05$.

FECDi compared with that in HCECi (Figs. 1B, 1C). Prolonged exposure to treatment with 0.5 mM tBHP resulted in $23.3 \pm 1.3\%$ of HCECi cells to enter early apoptosis and $36.8 \pm 0.1\%$ in FECDi ($P = 0.010$). Treatment with 1.0 mM tBHP resulted in $28.8 \pm 1.1\%$ apoptosis in HCECi and $39.3 \pm 0.4\%$ in FECDi ($P = 0.041$).

To test the hypothesis that increased reactive oxygen species (ROS) production plays an important role in CEC apoptosis in FECD, cellular release of hydrogen peroxide was assayed using the enzyme assay reagent (Amplex Red)/horseradish peroxidase system (Invitrogen). In addition to establishing a baseline of hydrogen peroxide release, HCECi and FECDi were treated with 500 μ M tBHP, and time-dependent release of ROS was measured. HCECi and FECDi corneal endothelial cells continuously produced H_2O_2 , as shown by a time-dependent increase in resorufin fluorescence (Fig. 2). Importantly, FECDi displayed a significantly higher release of ROS after 20, 40, and 60 minutes ($P = 0.0014$, $P = 0.0004$, and $P = 0.0003$, respectively) compared with HCECi. After treatment with tBHP, a significantly higher level of H_2O_2 was detected in the FECDi compared with that in treated HCECi after 20, 40, and 60 minutes ($P = 0.01$, $P = 0.0033$, and $P = 0.0023$, respectively). The rate of H_2O_2 release of HCECi after treatment with tBHP was similar to that of FECDi at baseline. However, treatment of FECDi with tBHP led to an even higher generation of H_2O_2 .

Normal CECs Are Resistant to Oxidative-Stress-Induced Apoptosis Ex Vivo

To discern whether normal and diseased endothelia display differential susceptibility to oxidative stress when attached to the native basement membrane, we investigated apoptotic cell death in an ex vivo setting. After treatment with 0.5 mM tBHP for 4 hours, normal CECs exhibited a significant increase in the

intensity of FITC-labeled 8-OHdG, from 0.20 ± 0.05 to 0.43 ± 0.04 arbitrary intensity units/cell ($P = 0.031$) (Fig. 3A). Prolonged exposure (18 hours) with tBHP did not result in a significant difference in oxidative DNA damage between treated and untreated groups because there was a baseline increase in oxidative DNA damage after incubation in media alone. Interestingly, an increase in oxidative DNA damage after exposure with tBHP did not result in apoptotic cell death in either the 4-hour or the 18-hour treatment groups (Fig. 3B). PI staining was performed and did not indicate necrotic cell death after treatment with 0.5 mM tBHP for 18 hours (Fig. 3C). Even an increase in the oxidant concentration (up to 1 mM) did not induce a significant amount of apoptosis and necrosis ex vivo (data not shown).

Increased Susceptibility of FECD Endothelium to Oxidative Stress Ex Vivo

Based on the findings from normal CECs, a 4-hour treatment with tBHP was used to evaluate endothelial cell response to oxidative injury in normal and FECD ex vivo samples. Indirect immunofluorescence was performed to compare the localization of 8-OHdG and TUNEL labeling in pre- and posttreatment groups. Figure 4 presents confocal images in which the z-series was collapsed onto a single-image plane. In untreated specimens (Fig. 4A), FECD endothelium exhibited speckled cytoplasmic distribution of 8-OHdG, which was present to a much lesser extent in normal controls. Densitometric analysis revealed higher baseline oxidative DNA damage in FECD compared with normal CECs ($P = 0.041$), confirming our previous findings.³ After treatment with tBHP, oxidative DNA damage significantly increased in both normal ($P = 0.031$) and FECD CECs ($P = 0.022$) from baseline. Normal CECs showed $1 \pm 1\%$ apoptosis pretreatment and $2 \pm 2\%$ posttreatment with tBHP. FECD CECs showed $28 \pm 9\%$ at baseline and $50 \pm 14\%$ after treatment with tBHP. Normal CECs were resistant to oxidant-induced apoptosis, as is evident by a negligible increase in TUNEL-positive cells (1%) after the treatment. However, FECD CECs showed a 21% increase in the number of TUNEL-labeled apoptotic cells after pro-oxidant treatment, and the difference in the change of TUNEL-positive cell numbers in FECD CECs compared with normal CECs was statistically significant ($P = 0.015$) (Fig. 4B).

Increased p53 Levels in FECD

To investigate potential regulators of the apoptotic cascade, baseline levels of p53 protein were compared between normal

and FECD CECs by Western blot analysis. Figure 5A shows a representative blot from normal and FECD samples and Figure 5B presents the densitometric analysis of four normal and four FECD donors. p53 protein level was on average twofold higher in FECD compared with that in normal CECs ($P = 0.002$).

Figure 5C presents immunofluorescence studies comparing localization of p53 in the endothelium of normal and FECD donors. Confocal images were taken of whole mounts in which the z-series was collapsed into a single-image plane. In normal tissue, no significant staining with p53 antibody was detected. Of interest, FECD specimens exhibited a significant amount of p53 staining that was, for the most part, localized to the nucleus of the cells. p53-positive cells were 66.6% of total cell population in FECD endothelium compared with 1.3% in normal controls ($P < 0.001$) (Fig. 5D).

To investigate endothelial cell response to oxidative injury, normal corneal endothelium was subjected to 0.5 mM tBHP for 4 hours, and indirect immunofluorescence was performed to examine the levels of phospho-p53 in CECs. Figure 6 presents confocal images of normal untreated (top row), normal treated with tBHP (middle row), and FECD (bottom row) CECs after staining with phospho-p53 antibody. After treatment with tBHP, there was an accumulation of the phospho-p53 in the cytosol of normal CECs, as previously described.^{9,10} In FECD, diffuse cytoplasmic staining with phospho-p53 was detected in the majority of the cells without exposure to the oxidative insults. Negative controls consisted of normal and FECD CECs incubated with secondary antibody only.

DISCUSSION

We previously reported that there is oxidant-antioxidant imbalance and accumulation of oxidized DNA lesions in FECD compared with normal CECs.³ In the present study, we have demonstrated that normal CECs are highly resistant to oxidative stress, whereas FECD endothelium is more susceptible to oxidative-stress-induced apoptosis. Apoptosis has been detected in FECD postkeratoplasty specimens^{1,2,11}; however, the etiology of apoptotic cell death in FECD has yet to be elucidated. This is the first report describing p53's central role in the cell death seen in FECD. Since currently there is no animal model available to study molecular mechanisms of FECD, we developed an experimental system using native FECD tissue samples and correlated the findings to the cell line data. Our model enables study of the effect of an oxidizing environment on diseased CECs, which could, in turn, be correlated with CEC loss during the progression of FECD.

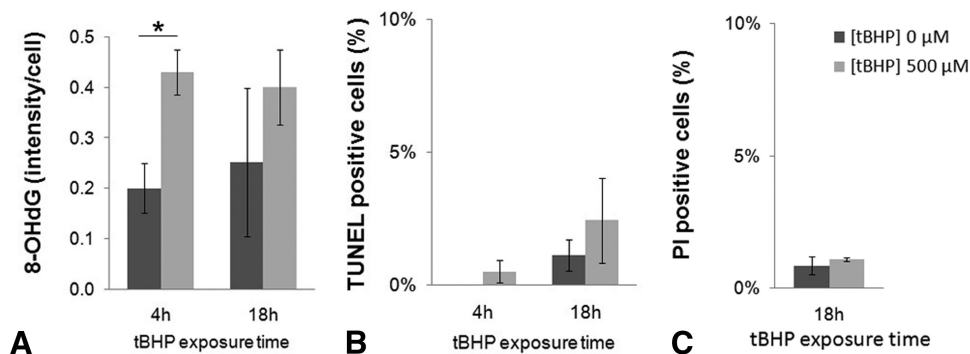


FIGURE 3. Normal CECs' resistance to oxidative stress induced by 500 μM tBHP. (A) Densitometric analysis of normal CECs labeled with anti-8-OHdG antibody reveals a significant increase in oxidative DNA damage after 4 hours, but not after 18 hours of tBHP treatment. Despite the increase in oxidative DNA damage, treatment of normal CECs with 500 μM tBHP did not result in significant apoptosis (TUNEL, B), and prolonged (18-hour) treatment with tBHP (C) did not cause significant necrosis (PI), suggesting that CECs are alive. Data are mean \pm SEM of tissue from three normal donors per condition (* $P = 0.031$).

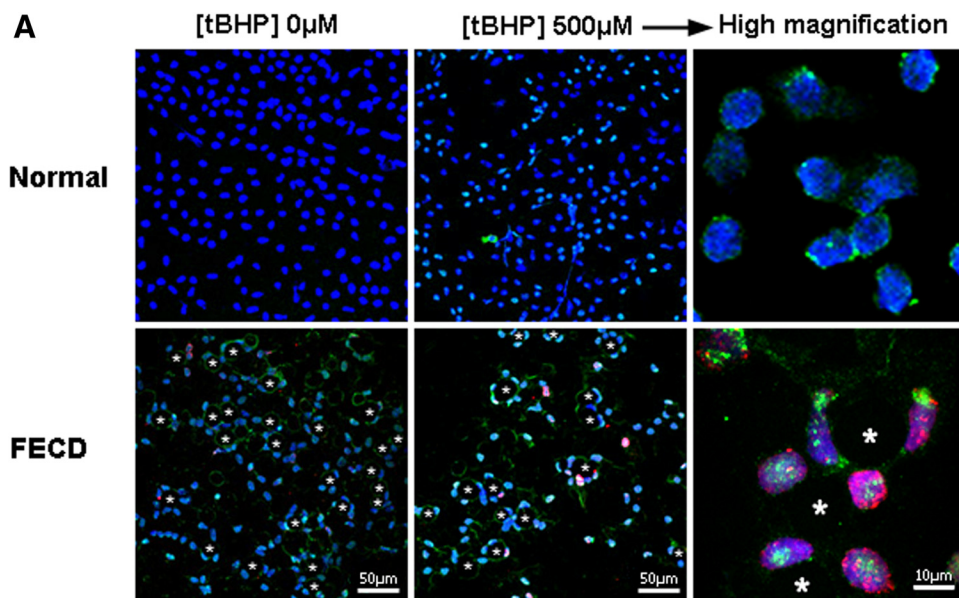
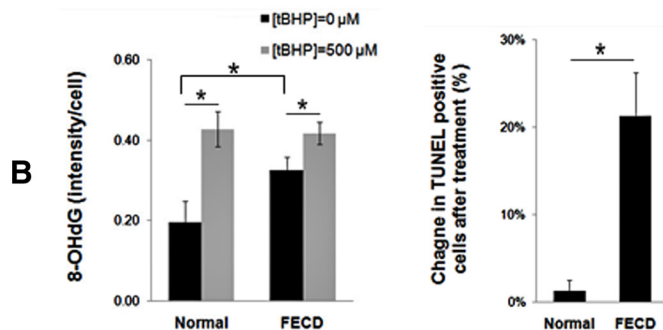


FIGURE 4. Normal and FECD endothelium treated with tBHP. (A) After treatment, specimens were labeled with TUNEL (red), anti-8-OHdG (green), and TOPRO-3 nuclear stain (blue). Asterisks mark the characteristic guttae of FECD corneal endothelium. Magnifications: $\times 400$ and $\times 630$ with $\times 6$ zoom. (B) Densitometric analysis shows increased levels of 8-OHdG staining in both normal and FECD specimens after treatment, with significantly increased TUNEL-positive staining in FECD ($*P < 0.05$). Data are mean \pm SEM of three normal and three FECD specimens.



FECD endothelium exhibits a significantly higher baseline oxidative DNA damage, which is low in normal cells. After pro-oxidant treatments, oxidative damage was heightened in both normal and FECD samples, but only FECD samples demonstrated an increase in apoptosis due to the increase in oxidative damage. We detected only a 1% increase in apoptosis in normal CECs after pro-oxidant treatments, whereas in FECD cells, apoptosis increased by 21%. Higher susceptibility of FECD CECs was also evident in the *in vitro* model because a higher level of apoptosis was seen in FECDi compared with that in HCECi after exposure to oxidative stress. In addition, ROS was produced at a significantly higher rate in FECDi than that in HCECi, indicating that apoptosis was indeed caused by intracellular ROS production. These findings suggest that there is an accumulation of oxidized DNA lesions in FECD CECs (possibly lifelong) and that they are present to a lesser degree in age-matched normal controls. In pro-oxidant conditions, the level of oxidative damage in normal CECs reaches the level seen in FECD. In this study, however, the oxidative insults were not sufficiently harmful to induce apoptosis in normal endothelium, whereas the FECD-affected cells rapidly progressed to the state of apoptosis after the same insults. It is very likely that a decreased antioxidant defense system in FECD renders CECs more susceptible to oxidative-stress-induced DNA damage, which in turn leads to dystrophic cell loss.

In addition to antioxidant defense, cells counteract the consequences of oxidative stress by activating p53-dependent pathways. p53 is a transcription factor that is activated in response to oxidative DNA damage and regulates a variety of genes that lead either to cell cycle arrest and DNA damage repair or apoptosis. On activation, p53 is first phosphorylated,

most commonly at Ser15, in cytosol, and then translocated into the nucleus to induce the expression of p53-associated genes.^{9,10} When ROS-induced damage in the cell is severe, DNA repair cannot be accomplished and p53 targets the cell for apoptosis.¹² In our study, we detected a twofold increase in p53 synthesis in FECD cells at baseline, concurrent with heightened oxidative damage and apoptosis. Immunocytochemistry studies detected an increase in nuclear colocalization of p53 in FECD specimens, whereas p53 was not detected in normal samples, underscoring the notion that normally levels of p53 in cells are very low but are upregulated in response to stress.¹³ In addition, we noted early accumulation of Ser15-phospho-p53 primarily in the cytoplasm of the majority of FECD cells at baseline, indicating the presence of early phosphorylation and activation of p53 before manifestation of late stages of apoptosis as seen by TUNEL staining. Thus, our findings suggest that p53 plays a central role in the cell death seen in FECD.

Previous studies showed that p53 has a higher expression in central than in peripheral human corneal endothelium,¹⁴ and that central endothelium has a lower proliferative capacity,¹⁵ pointing to p53's function in negatively controlling cell division. Since corneal endothelium *in vivo* has limited replicative capacity, which is further diminished in FECD, it is unclear what p53's role is in cell cycle control during the disease process. Therefore, it is most likely that the main role of p53 in FECD pathogenesis is in the induction of apoptosis in oxidatively damaged endothelium. In our previous study, we showed that, in FECD, there is decreased synthesis of antioxidant genes, and that Nrf2 is the major transcription factor required for activation of the antioxidants downregulated in

FECD.³ Under conditions of oxidative stress, Nrf2 binds the antioxidant response element (ARE) in the promoters of antioxidant genes, and causes transcriptional upregulation of antioxidants such as peroxiredoxins, thioredoxin reductases, and glutathione-dependent peroxidases. Interestingly, it has been recently shown that p53 suppresses the Nrf2-dependent transcription of ARE-dependent genes and that there is negative correlation between Nrf2 and p53 activity.¹⁶ Therefore, it will be important to investigate the cross-talk between Nrf2 and p53 in corneal endothelium and how it affects cell survival under normal and stressful conditions.

To summarize, in this study, we have shown that FECD corneal endothelium is susceptible to oxidative DNA damage, which in turn leads to apoptosis. There is heightened ROS

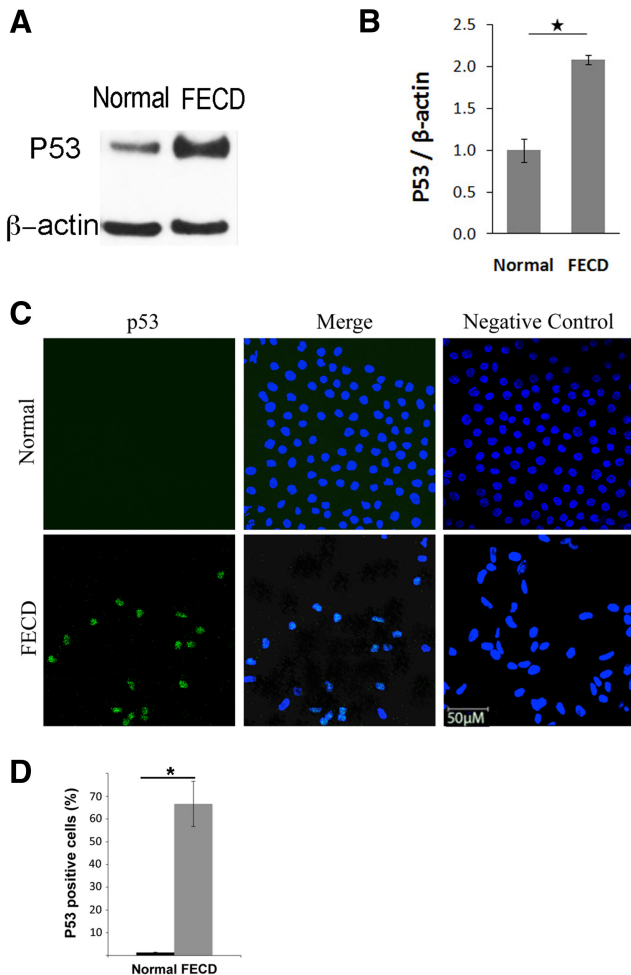


FIGURE 5. Increased p53 protein level in FECD compared with normal CECs. (A) A representative Western blot shows increased p53 levels in FECD compared with normal CEC. β -Actin was used for normalization of protein loading. (B) Densitometric analysis of p53 levels in CECs. Data are mean \pm SEM of four normal and four FECD specimens ($*P = 0.002$). (C) Representative confocal images of normal (top row) and FECD (bottom row) endothelium as whole mounts. Nuclear staining of p53 (green) was detected at a higher level in FECD samples compared with normal controls. TOPRO-3 was used for nuclei staining (blue). Overlay of the two channels showed colocalization of p53 and nuclear stain in FECD. Images of negative controls incubated with only secondary antibody are shown in the right column. (D) Densitometric analysis shows increased proportion of p53-positive cells in FECD compared with normal controls ($*P < 0.001$). Data are mean \pm SEM of three normal and three FECD specimens. Original magnification, $\times 400$ with $\times 2$ zoom.

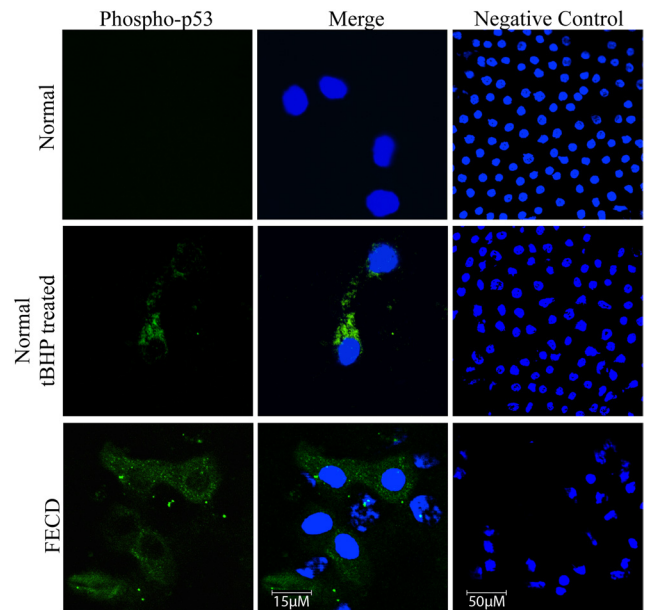


FIGURE 6. Representative confocal images of corneal endothelial whole mounts from normal (top row), normal treated with tBHP (middle row), and FECD (bottom row) specimens. Cytoplasmic localization of phospho-p53 (green) was present in normal endothelium after treatment with tBHP and in FECD specimens. TOPRO-3 was used for nuclei staining (blue). Images of negative controls incubated with only secondary antibody are shown in the right column. Original magnification was $\times 400$ with $\times 6$ zoom and $\times 2$ zoom in the first two rows and $\times 5$ zoom and $\times 3$ zoom in the third row.

production in FECD, further corroborating the fact that oxidative stress is a major cause of apoptosis in susceptible FECD endothelium. The mechanism leading to CEC death in FECD is unknown and remains subject to ongoing investigation. Furthermore, we have demonstrated increased levels of p53 in FECD endothelium and suggest that p53-mediated apoptosis may play a role in the cell death process. The complex interaction between the p53-regulated pathway and antioxidant defense, which is deficient in FECD, needs further investigation. Finally, the findings reported in this study give further support that enhancing the antioxidant defense and/or targeting p53-regulated pathways could play a relevant role in preventing the endothelial cell loss seen in FECD.

References

1. Borderie VM, Baudrimont M, Vallee A, Ereau TL, Gray F, Laroche L. Corneal endothelial cell apoptosis in patients with Fuchs' dystrophy. *Invest Ophthalmol Vis Sci.* 2000;41:2501-2505.
2. Li QJ, Ashraf MF, Shen DF, et al. The role of apoptosis in the pathogenesis of Fuchs endothelial dystrophy of the cornea. *Arch Ophthalmol.* 2001;119:1597-1604.
3. Jurkunas UV, Bitar MS, Funaki T, Azizi B. Evidence of oxidative stress in the pathogenesis of Fuchs endothelial corneal dystrophy. *Am J Pathol.* 2010;177:2278-2289.
4. Jurkunas UV, Rawe I, Bitar MS, et al. Decreased expression of peroxiredoxins in Fuchs' endothelial dystrophy. *Invest Ophthalmol Vis Sci.* 2008;49:2956-2963.
5. Joyce NC, Zhu CC. Human corneal endothelial cell proliferation: potential for use in regenerative medicine. *Cornea.* 2004;23:S8-S19.
6. Griffith M, Osborne R, Munger R, et al. Functional human corneal equivalents constructed from cell lines. *Science.* 1999;286:2169-2172.
7. He Y, Weng J, Li Q, Knauf HP, Wilson SE. Fuchs' corneal endothelial cells transduced with the human papilloma virus E6/E7 oncogenes. *Exp Eye Res.* 1997;65:135-142.

8. Chen CH, Rama P, Chen AH, et al. Efficacy of media enriched with nonlactate-generating substrate for organ preservation: in vitro and clinical studies using the cornea model. *Transplantation*. 1999; 67:800-808.
9. Liu J, Mao W, Ding B, Liang CS. ERKs/p53 signal transduction pathway is involved in doxorubicin-induced apoptosis in H9c2 cells and cardiomyocytes. *Am J Physiol Heart Circ Physiol*. 2008; 295:H1956-H1965.
10. She QB, Chen N, Dong Z. ERKs and p38 kinase phosphorylate p53 protein at serine 15 in response to UV radiation. *J Biol Chem*. 2000;275:20444-20449.
11. Szentmary N, Szende B, Suveges I. p53, CD95, cathepsin and survivin pathways in Fuchs' dystrophy and pseudophakic bullous keratopathy corneas. *Histol Histopathol*. 2008;23:911-916.
12. Vogelstein B, Lane D, Levine AJ. Surfing the p53 network. *Nature*. 2000;408:307-310.
13. Nair VD, McNaught KS, Gonzalez-Maeso J, Sealfon SC, Olanow CW. p53 mediates nontranscriptional cell death in dopaminergic cells in response to proteasome inhibition. *J Biol Chem*. 2006;281: 39550-39560.
14. Paul A, Whikehart D. Expression of the p53 family of proteins in central and peripheral human corneal endothelial cells. *Mol Vis*. 2005;11:328-334.
15. Joyce NC. Proliferative capacity of the corneal endothelium. *Prog Retin Eye Res*. 2003;22:359-389.
16. Faraonio R, Vergara P, Di Marzo D, et al. p53 suppresses the Nrf2-dependent transcription of antioxidant response genes. *J Biol Chem*. 2006;281:39776-39784.